NATIONAL AERONAUTICAL ESTABLISHMENT
LIBRARY

R. & M. No. 2527
(8372)
A.R.C. Technical Report

MINISTRY OF SUPPLY

AERONAUTICAL RESEARCH COUNCIL
REPORTS AND MEMORANDA

The Effect of Model Size on Measurements in the R.A.E. High Speed Tunnel. Drag of Two-dimensional Symmetrical Aerofoils at Zero Incidence

By

W. A. MAIR, M.A., and H. E. GAMBLE, B.Sc.

Royal Aircraft Establishment
6-APR 1951
LIBRARY

Crown Copyright Reserved

LONDON: HIS MAJESTY'S STATIONERY OFFICE
1951
THREE SHILLINGS NET

NATIONAL AERONAUTICAL ESTABLISHMENT
LIBRARY

The Effect of Model Size on Measurements in the R.A.E. High Speed Tunnel. Drag of Two-dimensional Symmetrical Aerofoils at Zero Incidence

By

W. A. MAIR, M.A., and H. E. GAMBLE, B.Sc.

COMMUNICATED BY THE PRINCIPAL DIRECTOR OF SCIENTIFIC RESEARCH (AIR), MINISTRY OF SUPPLY

Reports and Memoranda No. 2527*

December, 1944

Royal Aircraft Establishment
6 APR 1951
LIBRARY

Summary.—Pitot traverse drag measurements were made at zero incidence on three NACA 0015 aerofoils of different sizes. Pressures at the tunnel walls were also measured. For each aerofoil, tests were made at two different Reynolds numbers by changing the tunnel pressure. From the results it has been possible to separate the effects of varying Reynolds number and tunnel wall interference. It has been shown that the blockage corrections in current use (based on linear theory) are not large enough to equalise drag measurements made on different sizes of aerofoil at the same Reynolds number. Empirically increased corrections which bring the results into agreement have been found.

The results have also shown that at high Mach numbers there is a fairly large variation of drag coefficient with Reynolds number, especially between Reynolds numbers of about $0{\cdot}2 \times 10^6$ and $1{\cdot}4 \times 10^6$.

1. *Introduction.*—Measurements in flight at high speeds[1] have shown a less severe rise of aircraft drag with Mach number than has been shown by high-speed tunnel tests. Possible causes of this discrepancy are :—

(1) The difference of Reynolds number between tunnel and flight.

(2) The effect of the tunnel walls.

(3) The effect of turbulence in the tunnel.

The tests described in this report were made to investigate the first two of these causes. By varying both the tunnel pressure and the model size results were obtained for different sizes of model at the same Reynolds number, thus giving the variation of tunnel wall interference with model size. The effect of Reynolds number was investigated by changing the tunnel pressure, keeping the model size fixed.

The tests were made on two-dimensional aerofoils, partly to simplify the interpretation of the results and also because with three-dimensional models it is difficult to change the dimensions of the supporting system in the same ratio as the model dimensions.

2. *Description of Tests.*—The tests were made in the Royal Aircraft Establishment High Speed Tunnel during August, 1944. The models used were two-dimensional symmetrical aerofoils of NACA 0015 section, spanning the working section vertically. The chords of the aerofoils were

* R.A.E. Report No. Aero. 1998—received 24th January, 1945.

6 in., 15 in. and 37·5 in., and the length was 7 ft. in each case. The smallest aerofoil was made of steel, and the two larger ones were of hardwood. The position of the maximum thickness of each aerofoil was approximately on the centre-line of the balance, 5 ft. downstream from the start of the working section. The two smaller aerofoils were braced with steel wires to the sides of the tunnel, but these were arranged so that the wake from the wires passed clear of the pitot and static combs.* All the tests were made with the aerofoils at zero incidence. Ordinates of the aerofoil section are given in Table 1.

Tests were made at two Reynolds numbers on each aerofoil, a full range of Mach numbers being covered at each Reynolds number. The Reynolds numbers of the tests are given below.

Chord	*Reynolds Numbers*
6 in.	$0{\cdot}225 \times 10^6$ and $0{\cdot}55 \times 10^6$.
15 in.	$0{\cdot}55 \times 10^6$ and $1{\cdot}4 \times 10^6$.
37·5 in.	$1{\cdot}4 \times 10^6$ and $3{\cdot}4 \times 10^6$.

Thus for each of the Reynolds numbers $0{\cdot}55 \times 10^6$ and $1{\cdot}4 \times 10^6$ results were obtained for two sizes of model, enabling the effects of wall interference and Reynolds number to be separated.

The tests covered a range of Mach numbers up to the choking speed of the tunnel, except for the smallest aerofoil at $R = 0{\cdot}55 \times 10^6$, where the tunnel was not quite choked at the maximum permissible fan speed.

Drag was measured by the wake traverse method, the pitot and static measurements being made separately with different combs. The static comb was calibrated in the empty tunnel in two extreme positions. For most of the tests the wake traverses were made one chord behind the trailing edge, but the drag of the largest aerofoil at $R = 3{\cdot}4 \times 10^6$ was also measured with the comb only 4 in. behind the trailing edge to check the method of determining the drag.

Static pressures were measured at holes placed about half-way up the two vertical tunnel walls. These measurements were made for all the aerofoils with the static comb in position, and also for the two positions of the static comb with no aerofoil in the tunnel.

3. *Drag.*—The drag coefficients were computed from the wake traverses by the simplified method developed by Thompson.[2] A few of the drag coefficients at the highest Mach numbers were also computed by the more elaborate method of R. & M. 1971[3] in order to check the accuracy of the simplified method. The difference between the results of the two methods was never more than 1 per cent. The correction given in R. & M. 1971[3] for finite diameter of pitot tube was applied to all the results.

For a preliminary consideration of the results, the values of C_D and M were corrected by the blockage corrections normally used at present in reducing the results of high-speed tunnel tests. The equation used for calculating these corrections was

$$\varepsilon = \frac{0{\cdot}00075}{\beta^3}\left[C^2 + 37{\cdot}4\, C\, C_D\right], \quad .. \quad .. \quad .. \quad .. \quad (1)$$

where $\beta = \sqrt{1 - M^2}$, C = chord in feet and $\varepsilon = \frac{\Delta V}{V}$. These corrections are based on R. & M. 2033[4], but it should be noted that in equation (39) of that report β^2 has been replaced by β^3.

The results of the drag measurements, corrected in this way, are given in Figs. 1 to 6. These blockage corrections are based on the linear perturbation theory, which is not applicable when shock waves are present, but no more general theory is known at present.

* Later work has shown that the 'wake blockage' effect of these bracing wires may have been quite important, although it was assumed to be negligible at the time when the measurements were made.

Figs. 1 and 2 show that there is considerable scale effect on drag at high Mach numbers. In Fig. 3 there is a small scale effect.

The curves given in Figs. 1 to 3 are rearranged in Figs. 4 and 5 to show the effect of varying model size at constant Reynolds number. These curves show that, with the corrections used at present, the rise of C_D with M for a given Reynolds number is steeper for a large aerofoil than for a small one. If the blockage corrections were increased, the drag curves for different sizes of aerofoils at high Mach numbers could be made more nearly coincident. Possible increases of the blockage corrections will be considered later in this report. The scale effect will be discussed more fully after the blockage corrections have been modified in this way.

The differences of drag below the critical Mach number, shown in Figs. 4 and 5, are probably due to differences of surface finish. The difference is greatest in Fig. 5, where the drag of a steel aerofoil is compared with that of a wooden one. The increase of drag with Mach number, below the critical value, is greater for the steel aerofoil than for the wooden one. This suggests that on the steel aerofoil the transition point is fairly far back at low tunnel speeds, and moves forward with increasing speed because the tunnel turbulence increases. On the wooden aerofoil the transition point is probably further forward at low speeds, so that the possible forward movement with increasing speed is less than on the steel aerofoil.

Fig. 6 shows the results of drag measurements on the largest aerofoil at $R = 3{\cdot}4 \times 10^6$ for two different positions of the comb. Above the critical Mach number there is no appreciable difference between the two curves. At lower Mach numbers there is a small difference of drag, some of which is probably due to errors in the measurement of static pressure in the wake. The static comb used for these tests was not very satisfactory, and the results of the comb calibration were rather irregular. The static pressure of the free stream, used in computing the drag coefficient from the wake traverse, was that measured in the empty tunnel at the position of the wake traverse. It has been pointed out by Taylor[5] that there may be errors in drag measurements made by wake traverses far downstream in a wind tunnel, due to the static pressure gradient along the tunnel axis. Since this error would vary with the distance of the traverse behind the aerofoil, it may explain some of the discrepancy shown in Fig. 6. A further possible explanation may be that the roughness of the aerofoil increased between the two tests, the measurements at 4 in. behind the trailing edge being made before those at 37·5 in.

For the purpose of these tests, however, only the part of the drag curve above the critical Mach number is important, and in this region Fig. 6 shows no appreciable difference between the two curves.

It was noticed in every case that the choking speed for a given model was lower for the smaller Reynolds number. This effect was greatest for the 15-in. aerofoil, the choking Mach numbers (uncorrected for blockage) being 0·808 for $R = 0{\cdot}55 \times 10^6$ and 0·817 for $R = 1{\cdot}4 \times 10^6$. This change of tunnel choking speed with Reynolds number is probably caused partly by change of the tunnel wall boundary layer and partly by change of aerofoil drag and hence of wake width.

4. *Wall Pressures.*—If P_1 is the static pressure at a point on the tunnel wall in the presence of a model and P_0 is the static pressure at the same point in the absence of the model, then the increment of velocity at the wall due to the model is given by

$$\frac{\triangle V_w}{V} = \tfrac{1}{2}\left(\frac{P_0 - P_1}{\tfrac{1}{2}\rho V^2}\right), \quad \ldots \quad \ldots \quad \ldots \quad \ldots \quad \ldots \quad (2)$$

where ρ and V are density and velocity in the empty tunnel, and the pressure changes are assumed to be small.

The measured wall pressures have been converted to velocity increments by the above equation and plotted against distance along the tunnel axis in Figs. 7, 8 and 9. The velocity increment shown is in each case that due to the aerofoil only, not including the comb or its supports. The Mach numbers shown on the curves are not corrected for blockage. In calculating the velocity increments the mean of the pressures on the two vertical tunnel walls was used, but in all cases the difference between the two pressures was very small.

Figs. 8 and 9 show a large increase of velocity at the wall as the tunnel choking speed is approached. With the tunnel choked, the greatest local Mach number at the wall was about 0·93 in each case.

At the lower Reynolds number for each of the aerofoils the effect of lag in the pipes was more serious than was expected, and the scatter of the points giving the wall pressures was rather high. It was considered that any difference of wall pressure with Reynolds number would be obscured by experimental errors in the low Reynolds number tests. For this reason only the results for the higher Reynolds numbers are given in Figs. 7, 8 and 9, and only these results were used in estimating the blockage corrections.

5. *Tunnel Wall Interference.*—5.1. *General Considerations.*—It has been shown that, if the standard blockage corrections of R. & M. 2033[4] are applied, the drag curves for models of different sizes at the same Reynolds number do not agree at high Mach numbers (Figs. 4 and 5). This shows that further corrections for wall interference are required in order to reduce the results to free air conditions.

The effect of the tunnel walls may be considered in two parts :—

(*a*) Increase of speed at the model.

(*b*) Distortion of the flow round the model.

The first of these effects could be completely counteracted by applying suitable blockage corrections, giving an increase of effective tunnel speed. The second effect is more troublesome and cannot in general be counteracted in this way. For example, if the blockage corrections were increased to make the drag curves for models of different sizes agree, it might be found that the lift and moment curves did not agree. In order to investigate the effect of the tunnel walls in distorting the flow round the model, further tests are to be made in the High Speed Tunnel. Pressure distributions will be measured on the aerofoils described in this report, over a range of incidences and for the same Reynolds numbers and Mach numbers as in the present tests. The results of these future tests should show how much of the discrepancy between models of different sizes is due to distortion of the flow and how much is due to change of effective tunnel speed.

The possible effect on drag of the pressure gradient due to the aerofoil wake has been considered, using the measured wall pressures to estimate roughly the magnitude of this pressure gradient. For the 15-in. aerofoil at $R = 1{\cdot}4 \times 10^6$ and $M = 0{\cdot}817$ (uncorrected), the correction to C_D is not more than about 0·005, and for lower Mach numbers the correction is much smaller. A correction of this order is too small to make any appreciable difference to the curves in Figs. 4 and 5.

Until further information is available on the effect of the tunnel walls in distorting the flow round a model, we may assume for simplicity that the principal effect of the walls is an increase of effective tunnel speed.

5.2. *Blockage Corrections from Wall Pressures.*—The blockage effect for a model in the tunnel will be considered in two parts, the solid and wake blockages, as in R. & M. 2033.[4] The former is due to the model apart from its wake, and the latter is due to the wake. This subdivision of the total blockage effect into solid and wake components is probably not entirely satisfactory, because the effective shape of the aerofoil, and hence the solid blockage, may be modified by the extension of the wake at high Mach numbers. However, in any theoretical approach to the problem it is necessary to consider the solid and wake blockages separately.

It can be shown[4] that the velocity increment at the tunnel wall due to a two-dimensional aerofoil and its images is exactly three times the velocity increment at the aerofoil due to the images only. Further, it can be shown from the linear perturbation theory of compressible flow that this factor of 3 is unaffected by changes of Mach number within the limits of the theory, that is in the absence of shock waves. The factor of 3 applies only to the solid blockage effect ; it does not apply to the wake blockage.

The wake is represented in R. & M. 2033[4] by a distribution of sources over the rear half of the aerofoil associated with sinks at an infinite distance downstream. The velocity increment due to the wake and its images at a plane far downstream is then the same at all points of the tunnel cross-section. However, the velocity increment at the model due to the wake images is only about half the increment at a plane far downstream. (The exact value of this factor depends on the effective position of the sources in the aerofoil.) Thus to find the wake blockage effect at the model we may take the velocity increment measured at the wall at a point far downstream (where the solid blockage effect is zero) and divide this by two. It should be emphasised, however, that it may not be strictly correct to divide the downstream increment by 2, as it is not known whether the wake can be represented sufficiently accurately by a system of sources or what are the positions of these sources in the aerofoil.

Now consider the interpretation of a typical curve, such as that in Fig. 10, showing the variation along the tunnel wall of the velocity increment due to the aerofoil. The full line shows the total velocity increment at the wall, as obtained from the observed wall pressures. The dotted lines show how this total velocity increment may be divided into solid and wake components. If the velocity increment at the wall at a point far downstream is denoted by B, the wake blockage effect at the model will be approximately $B/2$. If the maximum velocity increment at the wall is A, the increment due to the solid blockage only will be approximately $A-(B/2)$. This relation is not exact, because the peaks of the solid blockage curve and of the total velocity-increment curve do not necessarily occur at the same point. However, with these approximations, the blockage effects at the model are given by

$$\varepsilon \text{ (solid} = \tfrac{1}{3}\left(A - \frac{B}{2}\right),$$

$$\varepsilon \text{ (wake)} = \frac{B}{2},$$

$$\text{therefore} \quad \varepsilon \text{ (total)} = \tfrac{1}{3}\,(A + B),$$

where $\varepsilon = \dfrac{\Delta V}{V}$ at the model.

Using these relations, the blockage corrections for the three aerofoils have been calculated from the curves given in Figs. 7, 8 and 9. These blockage corrections are shown plotted against Mach number in Figs. 11, 12 and 13, together with the theoretical values from equation (1). For Mach numbers up to 0·7 the total blockage correction calculated from the wall pressures never differs by more than 0·006 from the theoretical value. For higher Mach numbers the increase of blockage given by the wall pressures is considerably greater than that given by the theory, and for the larger aerofoils this difference is mainly in the solid blockage. The wall pressures show a large increase of solid blockage as the choking speed is approached.

The blockage corrections deduced from the wall pressures, as given in Figs. 11, 12 and 13, have been used to correct the drag measurements. The corrected curves are given in Figs. 14 and 15. In calculating the blockage corrections only the wall pressures for the higher Reynolds number for each aerofoil have been used, for reasons already explained. The blockage corrections for the lower Reynolds numbers have been calculated on the assumptions that the solid blockage is independent of Reynolds number and that the wake blockage is directly proportional to the drag coefficient.

Figs. 14 and 15 show that, while these blockage corrections give better agreement than the corrections based on Ref. 4, a further increase of blockage corrections would be necessary to equalize drag measurements made on different sizes of aerofoil at the same Reynolds number. As discussed already, part of the discrepancy shown in Figs. 14 and 15 may be due to distortion of the flow by the tunnel walls, and further tests are proposed to investigate this. In the meantime, it may be useful to consider whether an empirical increase of blockage corrections will bring the drag curves into agreement.

5.3. *Modified Blockage Corrections.*—The effect of multiplying all the blockage corrections as given in Figs. 11, 12 and 13 by a constant factor was considered. If this factor was adjusted to make the results for the two smaller aerofoils agree, then it was found that the results for the largest aerofoil were over-corrected. This showed that the increase of blockage corrections should be proportionately greater for the smaller aerofoils than for the larger ones. The simplest way of satisfying this requirement empirically was to increase the wake blockage only, since the wake blockage is relatively more important for the smaller aerofoils.

It was assumed for this purpose that the wake and solid blockages were given by

$$\varepsilon \text{ (wake)} = B,$$

$$\varepsilon \text{ (solid)} = \tfrac{1}{3}(A - B),$$

where B is the velocity increment at the wall far downstream. That is, in the expressions originally used, B has been substituted for $B/2$. As before, it was assumed that the solid blockage was independent of Reynolds number and that the wake blockage was directly proportional to the drag coefficient. The drag curves corrected in this way are shown in Figs. 16 and 17. This arbitrary method of correcting for the effect of the tunnel walls appears to be fairly satisfactory for the particular measurements considered in this report.

It has been pointed out that the solid blockage correction, as given by the wall pressures, rises sharply as the choking speed of the tunnel is approached, and also that the choking speed for a given aerofoil increases with Reynolds nnmber. Thus the assumption that the solid blockage correction is independent of Reynolds number may not be accurate. In order to investigate the possible effect of this, the blockage corrections for each aerofoil at the lower Reynolds number were recalculated, assuming that the solid blockage rose to a fixed peak value at the choking speed, this peak value being independent of Reynolds number. This change in the method of calculating the blockage corrections was found to have a negligible effect on the drag curves.

Further small modifications to the blockage corrections were introduced to make the drag curves in Figs. 16 and 17 agree exactly. This was necessary to simplify the discussion of scale effect, considered later. The curve for the 15-in. aerofoil at $R = 0{\cdot}55 \times 10^6$ in Fig. 17 was moved to make it agree with that for the 6-in. aerofoil at the same Reynolds number. The same corrections were then applied to the results for the 15-in. aerofoil at $R = 1{\cdot}4 \times 10^6$. The results for the 37·5-in. aerofoil were then corrected to bring them into agreement with the corrected results for the 15-in. aerofoil. All these corrections refer only to Mach numbers above the critical value.

In order to show the effect of varying the blockage corrections on the drag curve of a model of the usual size, curves are shown in Fig. 18 for the 15-in. aerofoil at $R = 1{\cdot}4 \times 10^6$ with alternative methods of correcting for blockage. The curve marked " revised blockage corrections " refers to the blockage corrections required to make the drag curves in Figs. 16 and 17 agree. Fig. 18 shows that the effect on the drag curve of even the greatest blockage correction considered is fairly small, the increase of Mach number being only about 0·03 at a drag coefficient of three times the low-speed value.

Although empirical blockage corrections have been introduced which bring drag curves on different sizes of models into agreement, these corrections cannot be accepted as a final solution until further tests have been made to investigate the relative importance of distortion and blockage effects.

6. *Scale Effect.*—Before considering the effect of Reynolds number on the drag it is necessary to apply corrections to the results to remove, as far as possible, differences due to variations of wall interference and model roughness. In Figs. 16 and 17 the curves for models of different sizes at the same Reynolds number coincide at the Mach numbers at which the drag rises sharply. It is assumed that all drag differences below this Mach number are due to differences of surface roughness and that all differences at higher Mach numbers are due to wrong corrections for wall interference. The method of modifying the corrections to bring the drag curves into agreement above

the critical Mach number has already been explained. Below the critical Mach number the results have all been corrected to the appropriate values for the 15-in. aerofoil, using the differences shown in Figs. 16 and 17. It appears from the results that the transition point was further forward on the 15-in. aerofoil than on the other two aerofoils.

The drag curves, corrected for wall interference and reduced to a common standard of surface finish as described above, are shown in Fig. 19. This diagram shows that, at high Mach numbers, there is a considerable scale effect on drag. This scale effect is also shown in Figs. 20, 21 and 22 in which drag critical Mach number, drag coefficient and drag factor are plotted against (log R). The drag factor is defined as the ratio of C_D at high Mach number to C_D at $M = 0{\cdot}3$. The complete set of curves in Fig. 19 shows that there is only a small scale effect at Reynolds numbers above about $1{\cdot}4 \times 10^6$, but there is a fairly large scale effect at lower Reynolds numbers.

7. *Conclusions.*—It has been shown that, if blockage corrections based on Ref. 4 are used, the drag of a large aerofoil appears to rise more steeply with Mach number than that of a smaller aerofoil at the same Reynolds number. This means either that these blockage corrections are too small or that there is a serious distortion effect due to the tunnel walls which increases the drag at high Mach numbers.

Using empirically increased blockage corrections based on the observed wall pressures, the drag curves for models of different sizes at the same Reynolds number can be brought into agreement. However, these corrections cannot be accepted as a final solution until further tests have been made to investigate the relative importance of blockage and distortion effects.

There is a fairly large scale effect on drag at high Mach numbers, especially between Reynolds numbers of about $0{\cdot}2 \times 10^6$ and $1{\cdot}4 \times 10^6$. At higher Reynolds numbers the scale effect appears to be fairly small.

REFERENCES

No.	*Author*	*Title, etc.*
1	R. Smelt, W. J. Charnley and R. Rose.	Drag and Trim Changes on Spitfire, Mustang and Thunderbolt in Flight at High Mach Numbers. A.R.C. 7424. January, 1944.
2	J. S. Thompson	A Simple Method of Computing C_D from Wake Traverses at High Speeds. A.R.C. 8462. December, 1944.
3	C. N. H. Lock, W. F. Hilton and S. Goldstein.	Determination of Profile Drag at High Speeds by a Pitot Traverse Method. R. & M. 1971. September, 1940.
4	A. Thom	Blockage Corrections in a Closed High Speed Tunnel. R. & M. 2033. November, 1943.
5	G. I. Taylor	The Determination of Drag by the Pitot-Traverse Method. R. & M. 1808. November, 1937.

TABLE 1

Ordinates of NACA 0015 Aerofoil

Distance from leading edge	0	1·25	2·5	5·0	7·5	10·0	15	20	25
Half thickness	0	2·367	3·268	4·443	5·249	5·852	6·680	7·170	7·424
Distance from leading edge	30	40	50	60	70	80	90	95	100
Half thickness	7·500	7·252	6·615	5·703	4·579	3·278	1·809	1·008	0·157

Leading edge radius = 2·48.

All the above dimensions are expressed as percentages of the chord.

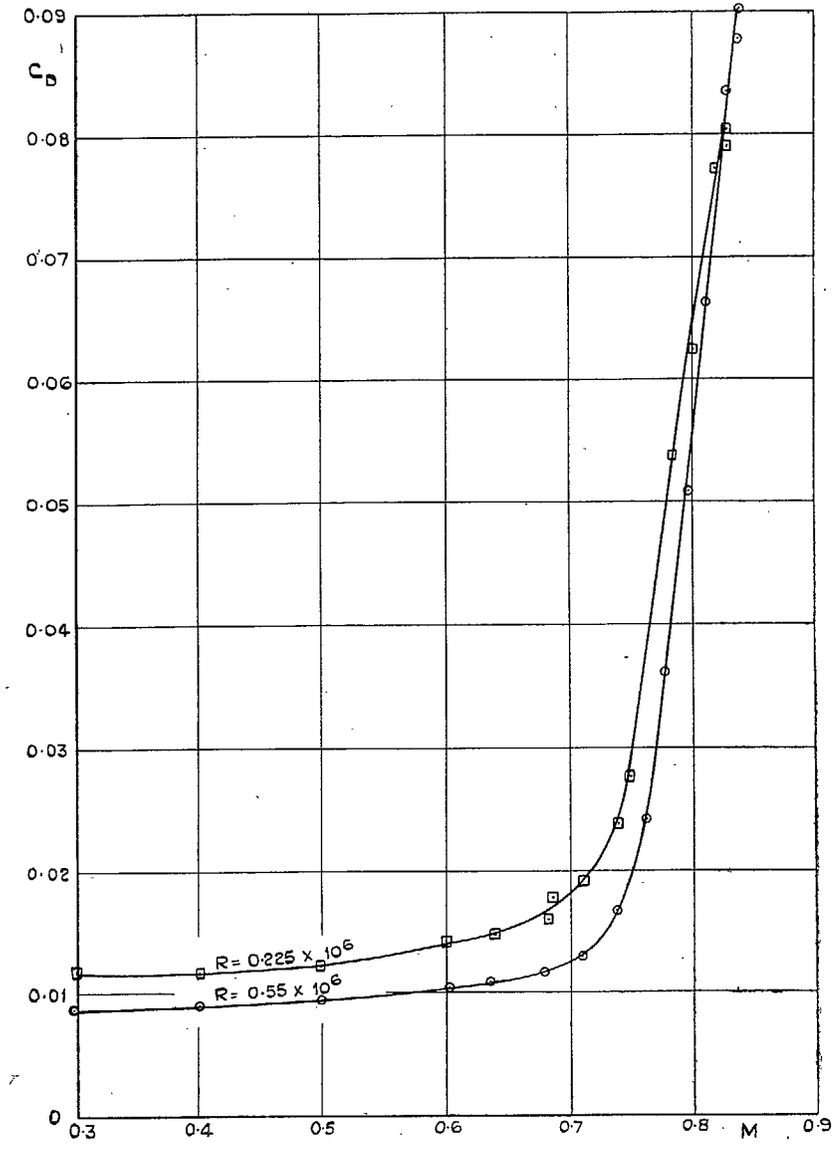

FIG. 1. Drag of 6-in. Chord Aerofoil NACA 0015 at Two Reynolds Numbers.—Incidence = 0 deg. Standard blockage corrections applied (equation (1)).

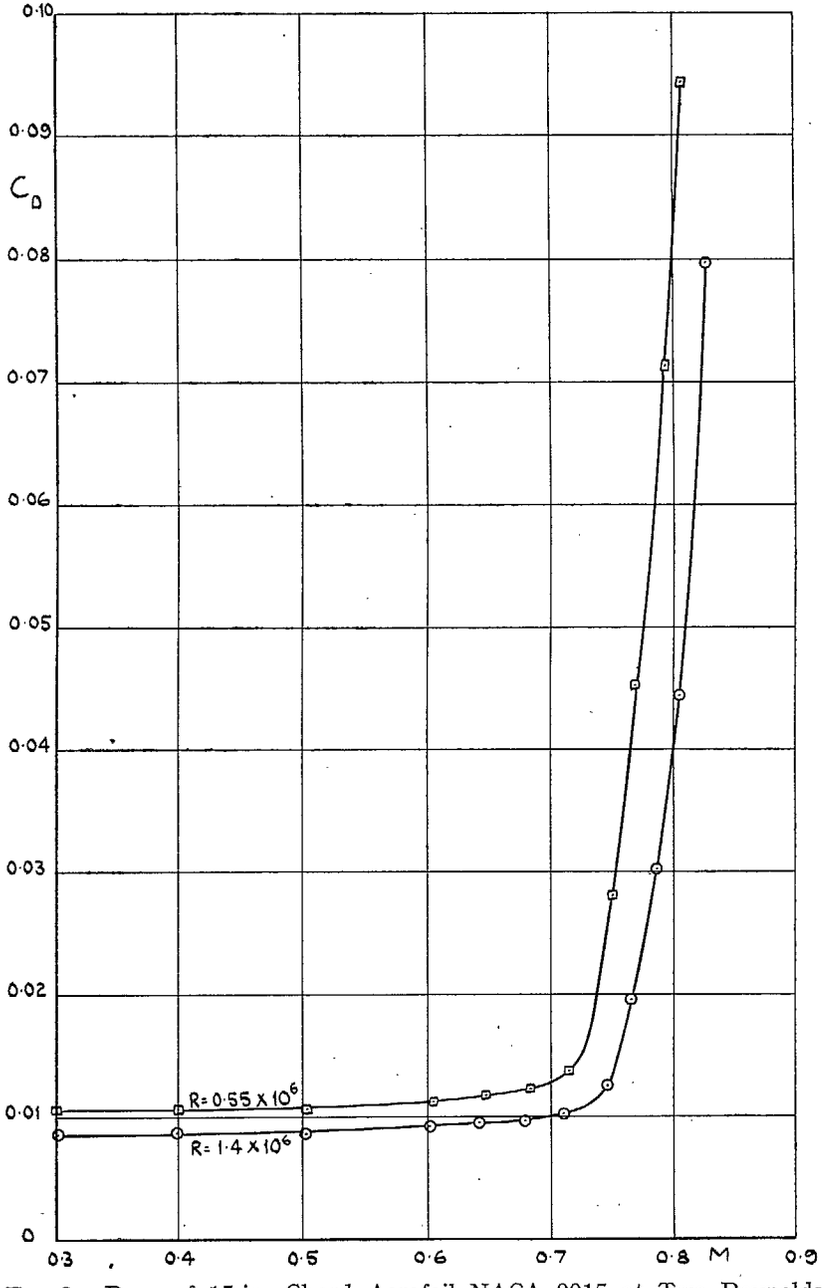

FIG. 2. Drag of 15-in. Chord Aerofoil NACA 0015 at Two Reynolds Numbers.—Incidence = 0 deg. Standard blockage corrections applied (equation (1)).

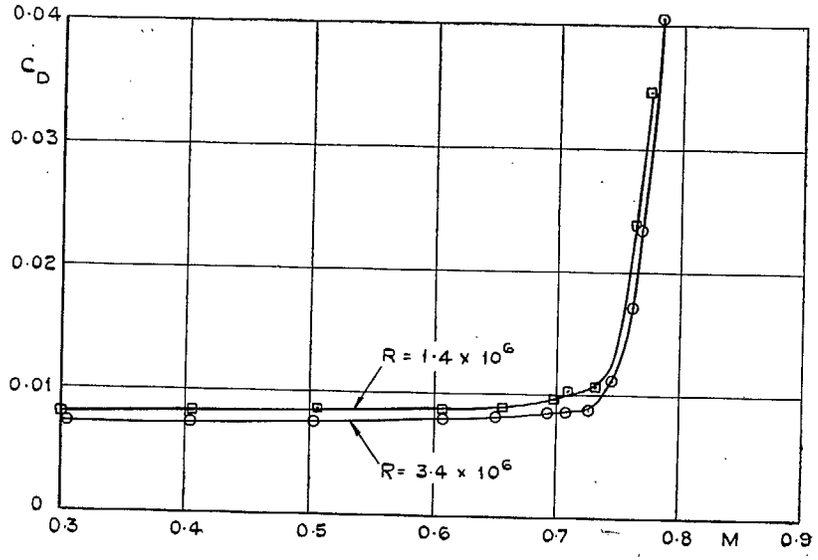

FIG. 3. Drag of 37·5-in. Chord Aerofoil NACA 0015 at Two Reynolds Numbers.—Incidence = 0 deg. Standard blockage corrections applied (Equation (1)).

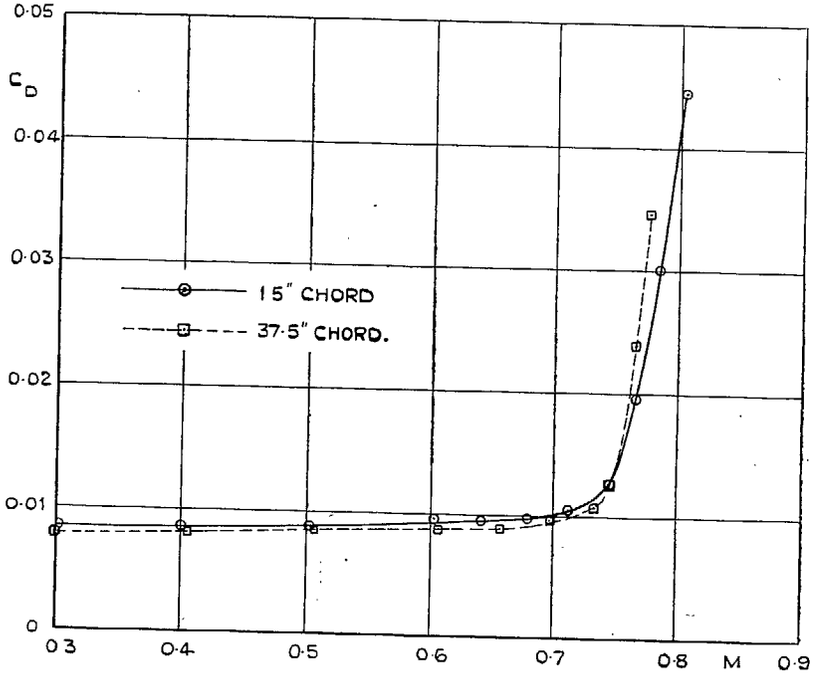

FIG. 4. Drag of NACA 0015 Aerofoils of Different Sizes. Incidence = 0 deg. $R = 1{\cdot}4 \times 10^6$. Standard blockage corrections applied (Equation (1)).

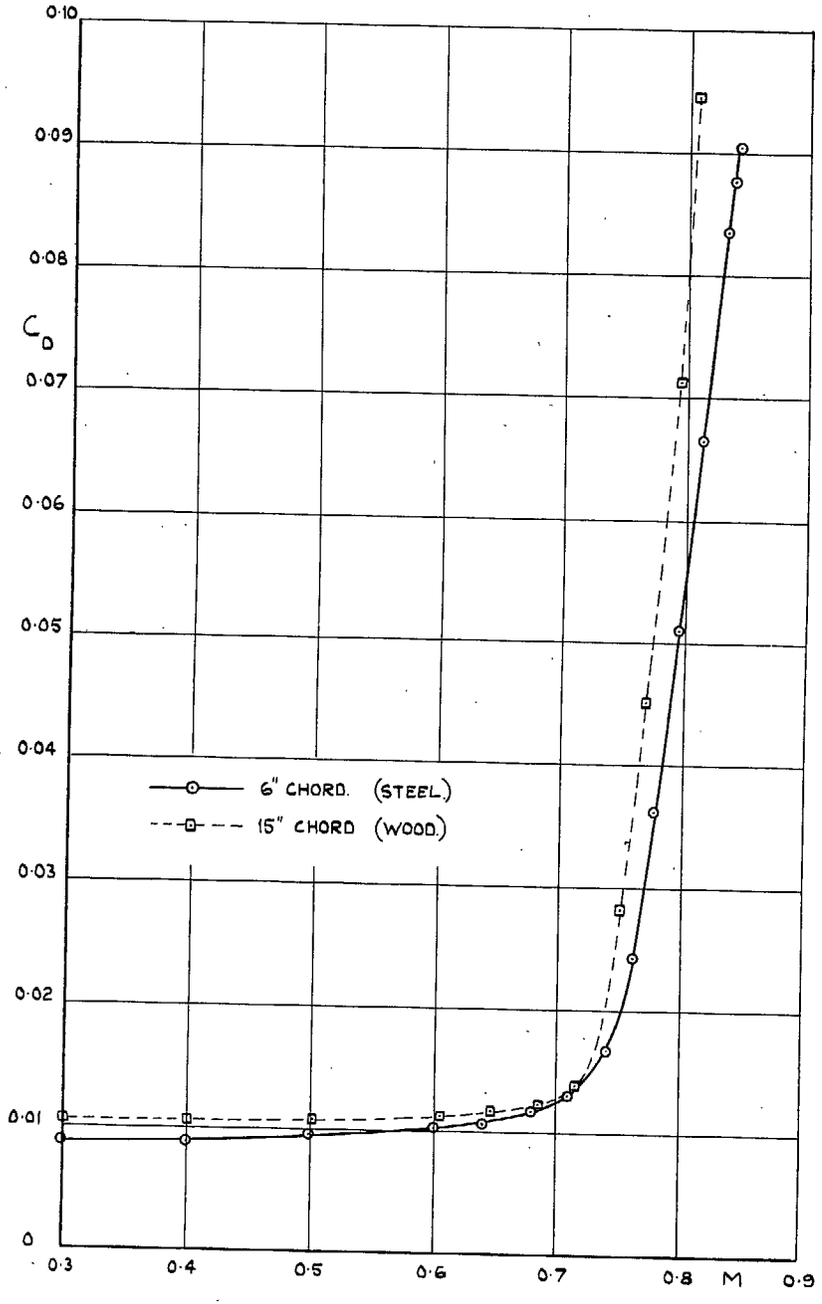

FIG. 5. Drag of NACA 0015 Aerofoils of Different Sizes. Incidence = 0 deg. $R = 0{\cdot}55 \times 10^6$. Standard blockage corrections applied (Equation (1)).

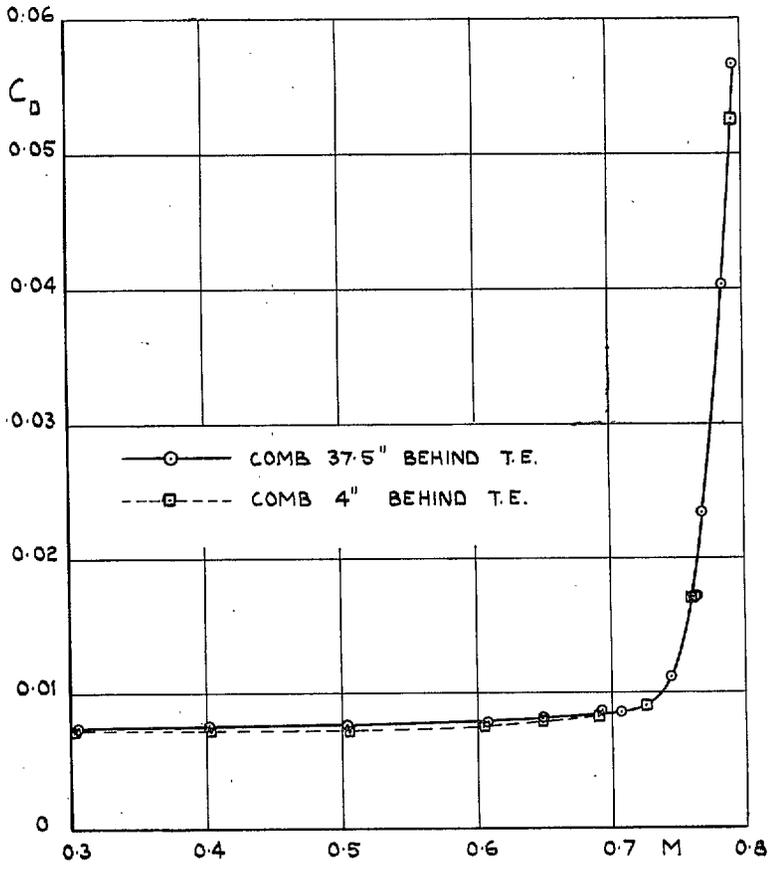

FIG. 6. Drag of 37·5-in. Chord Aerofoil NACA 0015. Incidence = 0 deg. $R = 3{\cdot}4 \times 10^6$. Comparison of Results for Different Positions of Comb. Standard blockage corrections applied (Equation (1)).

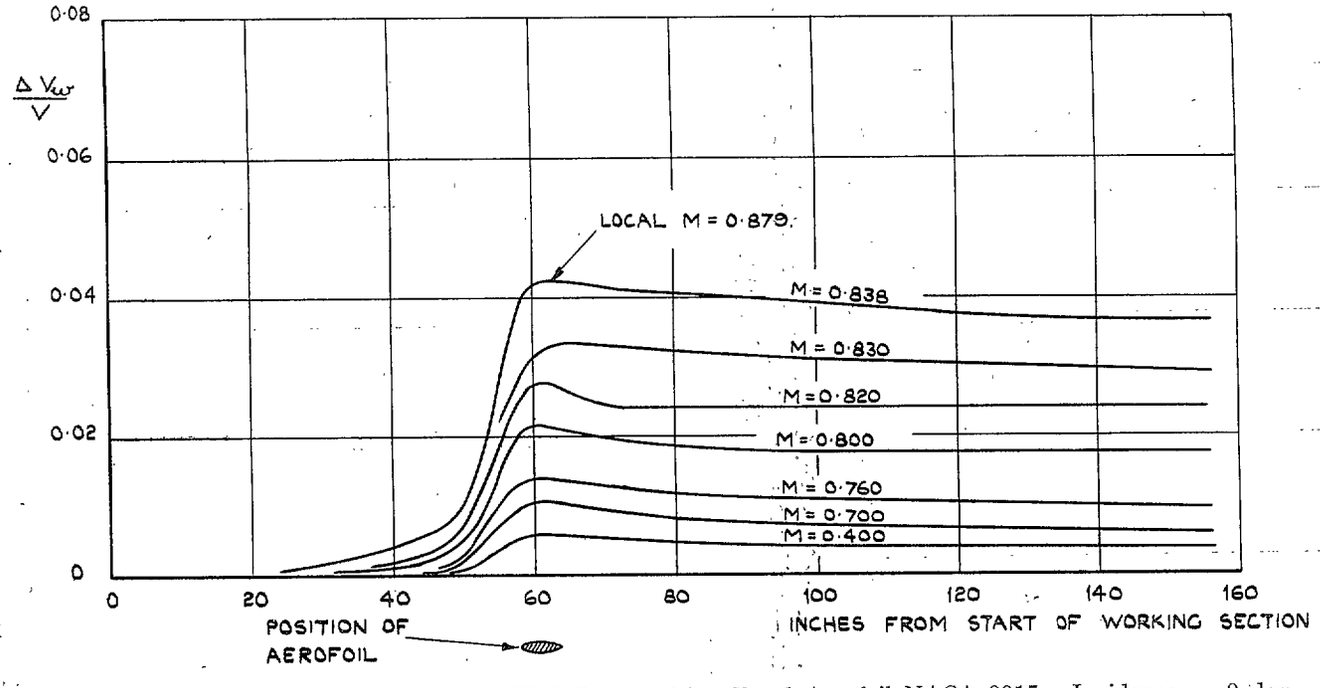

FIG. 7. Velocity Increment at Tunnel Wall Due to 6-in. Chord Aerofoil NACA 0015. Incidence = 0 deg. $R = 0{\cdot}55 \times 10^6$.

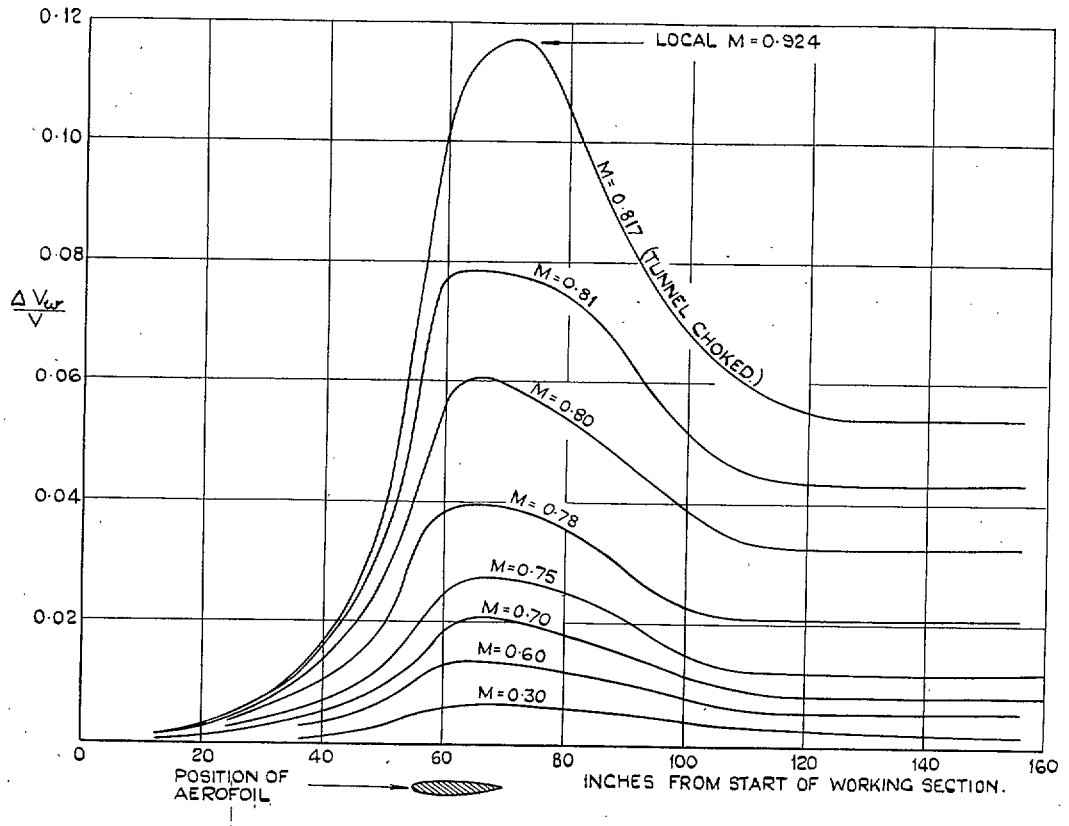

FIG. 8. Velocity Increment at Tunnel Wall Due to 15-in. Chord Aerofoil NACA 0015. Incidence = 0 deg. $R = 1{\cdot}4 \times 10^6$.

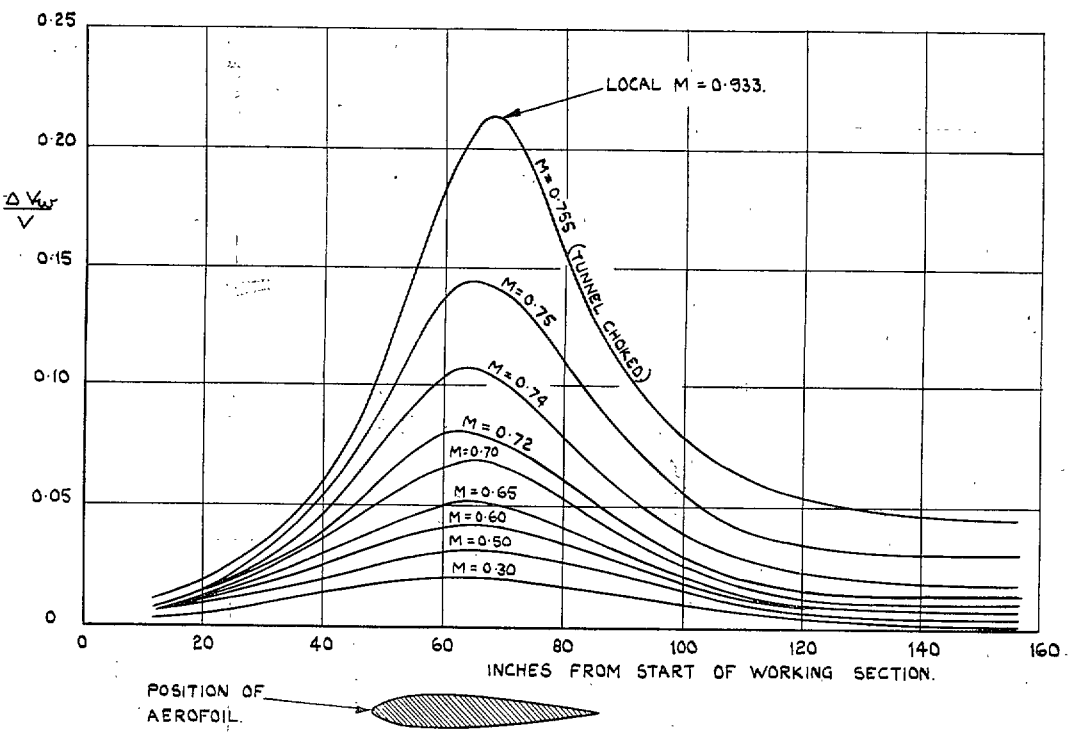

FIG. 9. Velocity Increment at Tunnel Wall Due to 37·5-in. Chord Aerofoil NACA 0015. Incidence = 0 deg. $R = 3{\cdot}4 \times 10^6$.

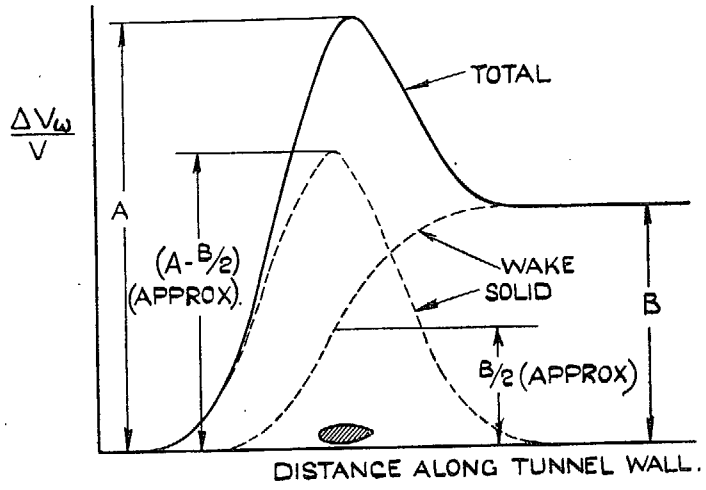

FIG. 10. Typical Curves Showing Variation along Tunnel Wall of Velocity Increments Due to Aerofoil.

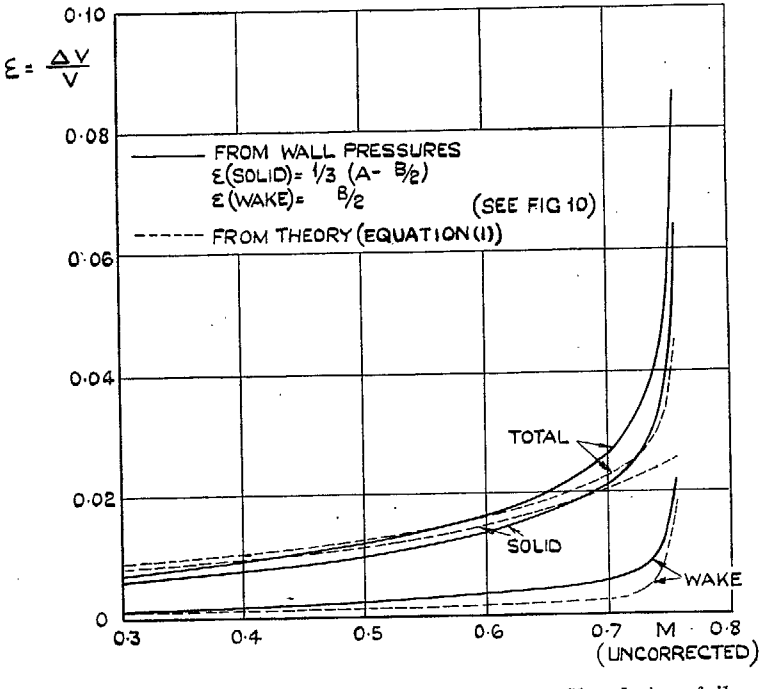

FIG. 11. Blockage Corrections for 37·5-in. Chord Aerofoil. $R = 3{\cdot}4 \times 10^6$.

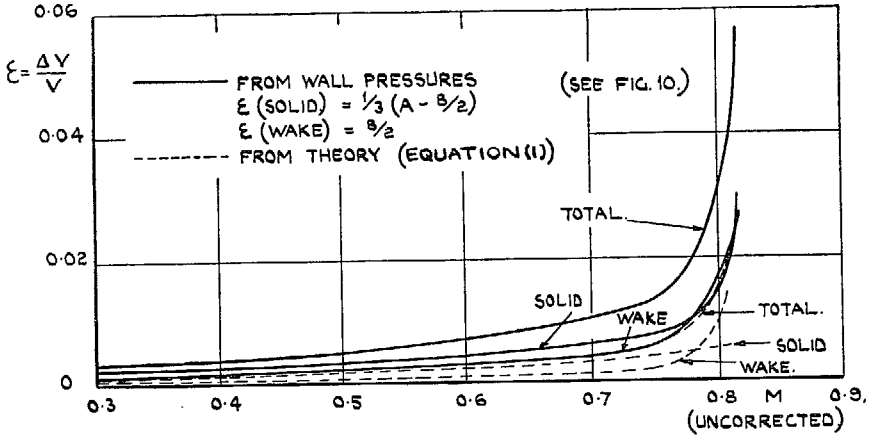

FIG. 12. Blockage Corrections for 15-in. Chord Aerofoil. $R = 1{\cdot}4 \times 10^6$.

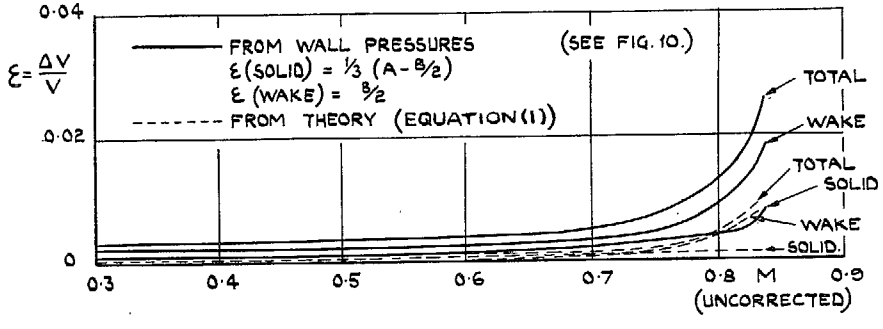

FIG. 13. Blockage Corrections for 6-in. Chord Aerofoil. $R = 0{\cdot}55 \times 10^6$.

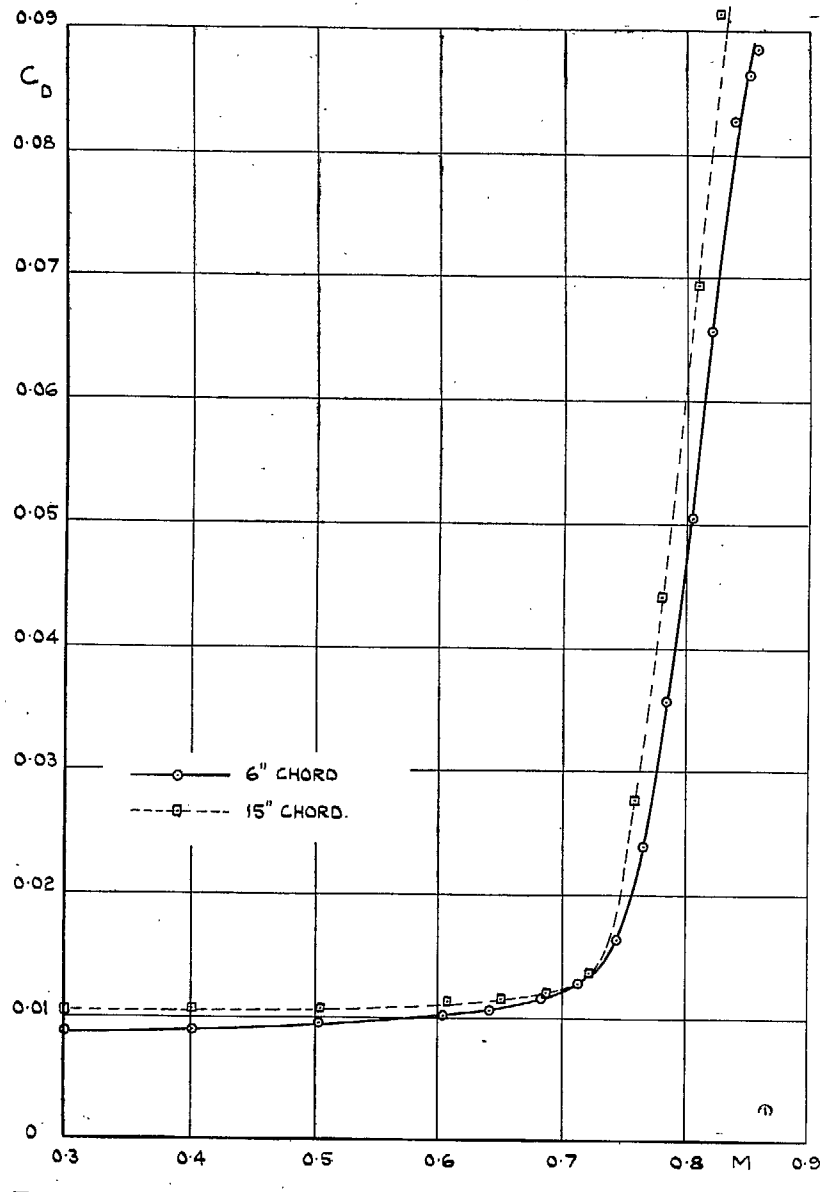

FIG. 14. Drag of Aerofoils at $R = 0{\cdot}55 \times 10^6$. Blockage from Wall Pressures (Figs. 12 and 13). ε (solid) $= \frac{1}{3}\left(A - \frac{B}{2}\right)$; ε (wake) $= \frac{B}{2}$ (Fig. 10).

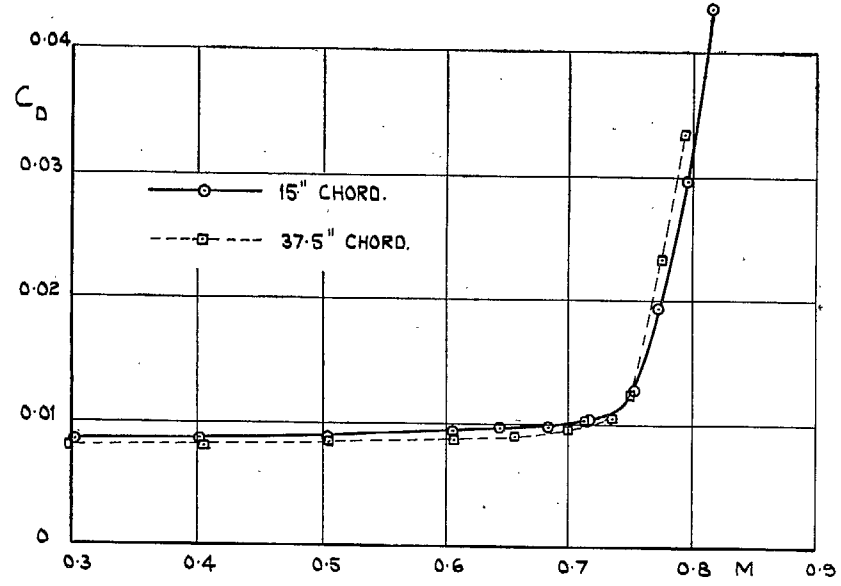

FIG. 15. Drag of Aerofoils at $R = 1{\cdot}4 \times 10^6$. Blockage from Wall Pressures (Figs. 11 and 12). ε (solid) $= \frac{1}{3}\left(A - \frac{B}{2}\right)$; ε (wake) $= \frac{B}{2}$ (Fig. 10).

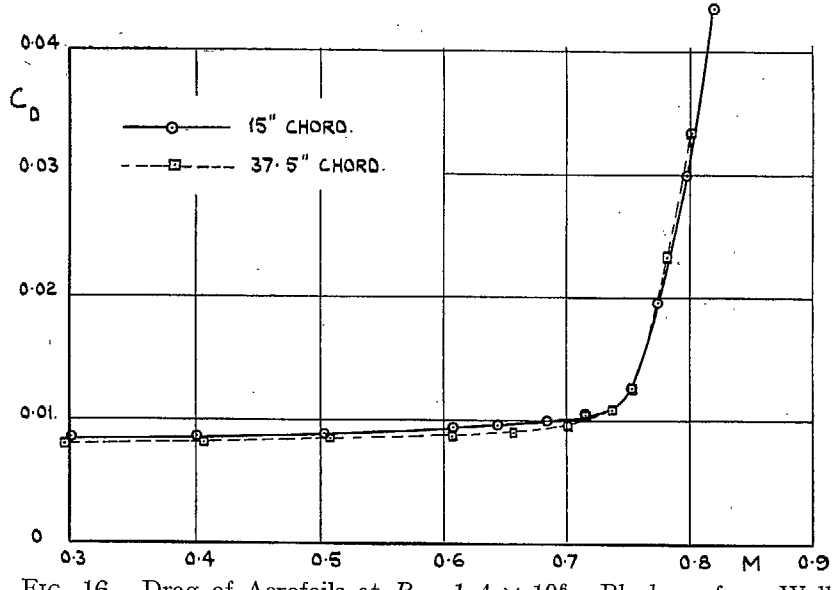

FIG. 16. Drag of Aerofoils at $R = 1{\cdot}4 \times 10^6$. Blockage from Wall Pressures with Wake Effect Doubled. ε (solid) $= \frac{1}{3}(A - B)$; ε (wake) $= B$ (Fig. 10).

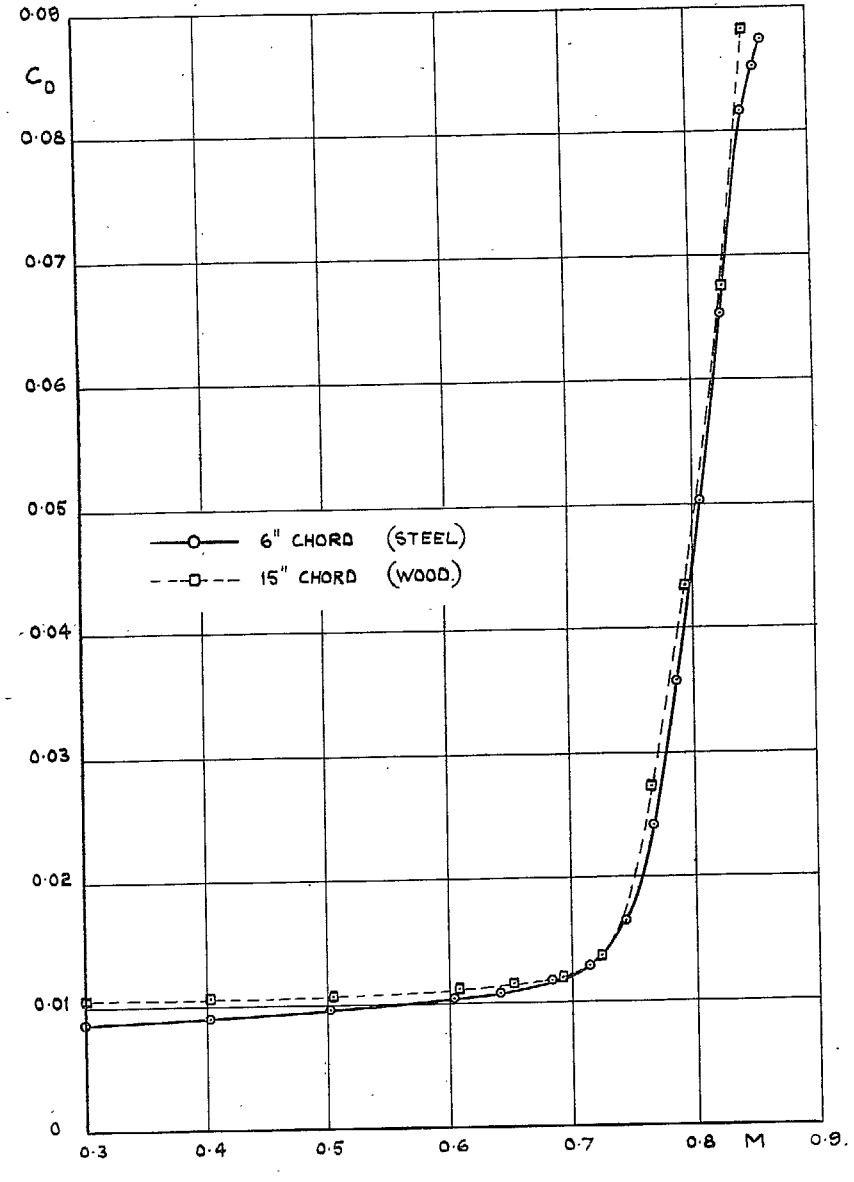

FIG. 17. Drag of Aerofoils at $R = 0{\cdot}55 \times 10^6$. Blockage from Wall Pressures with Wake Effect Doubled. ε (solid) $= \frac{1}{3}(A - B)$; ε (wake) $= B$ (Fig. 10).

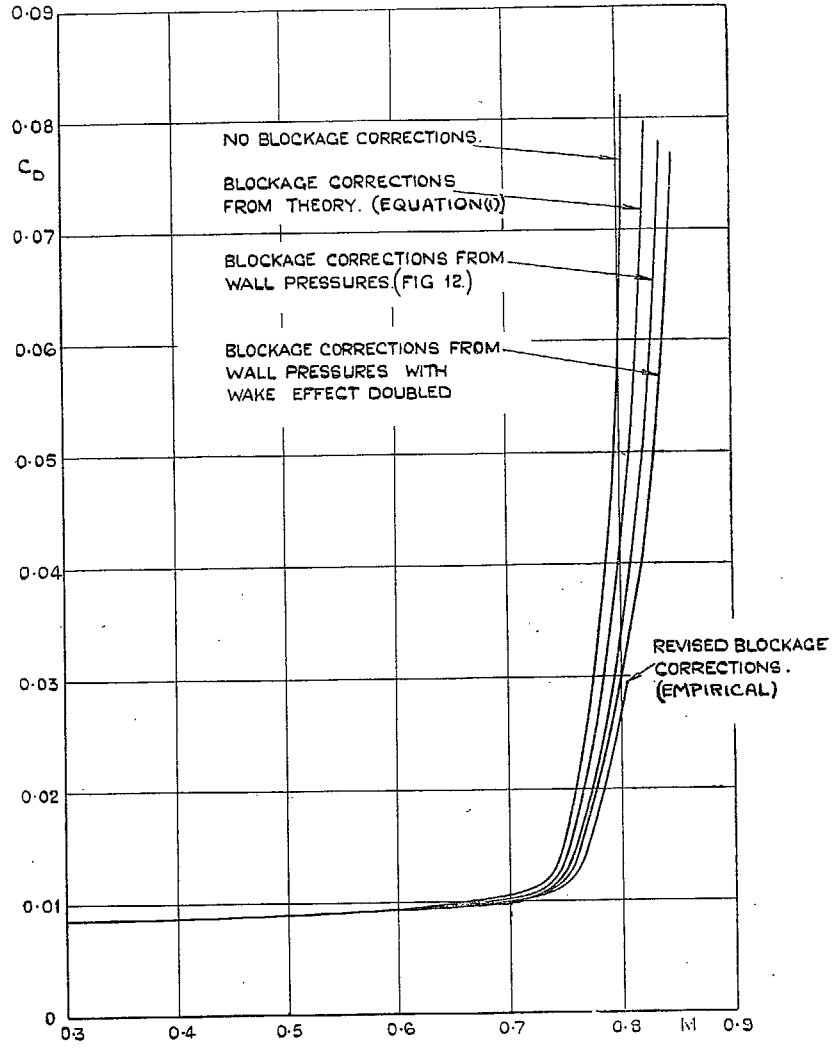

FIG. 18. Drag of 15-in. Chord Aerofoil NACA 0015. $R = 1{\cdot}4 \times 10^6$. Effect of Alternative Blockage Corrections.

(93017) Wt. 13/806 K.5 2/51 Hw.

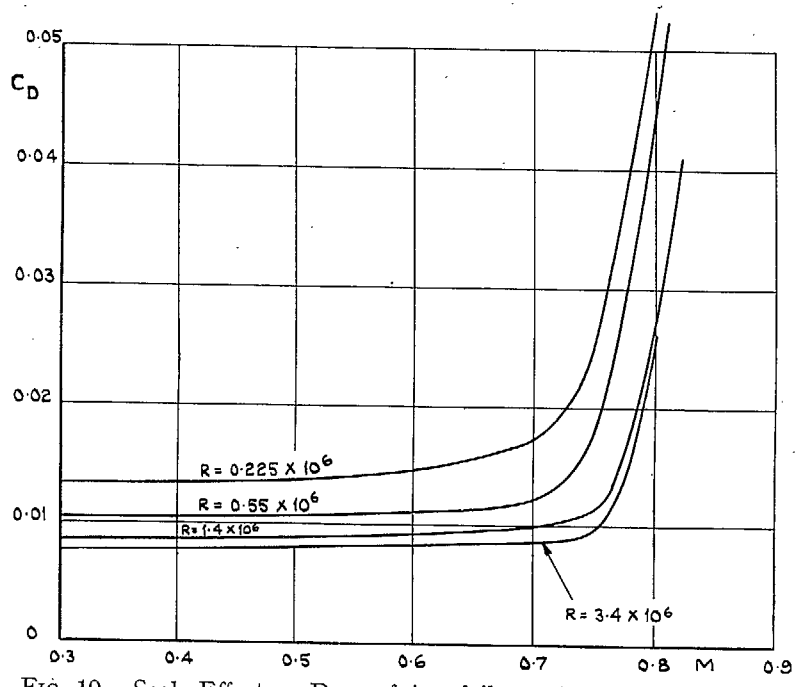

FIG. 19. Scale Effect on Drag of Aerofoil at High Mach Numbers. NACA 0015 at Zero Incidence.
(All results fully corrected for wall interference.)

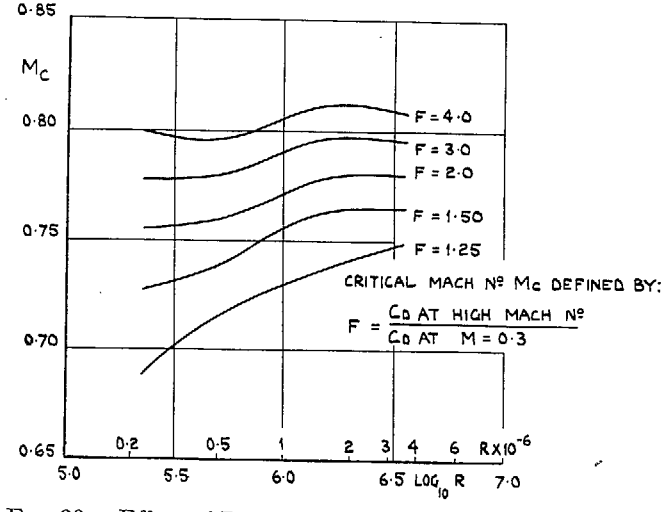

FIG. 20. Effect of Reynolds Number on Drag Critical Mach Number. (Results fully corrected for wall interference.)

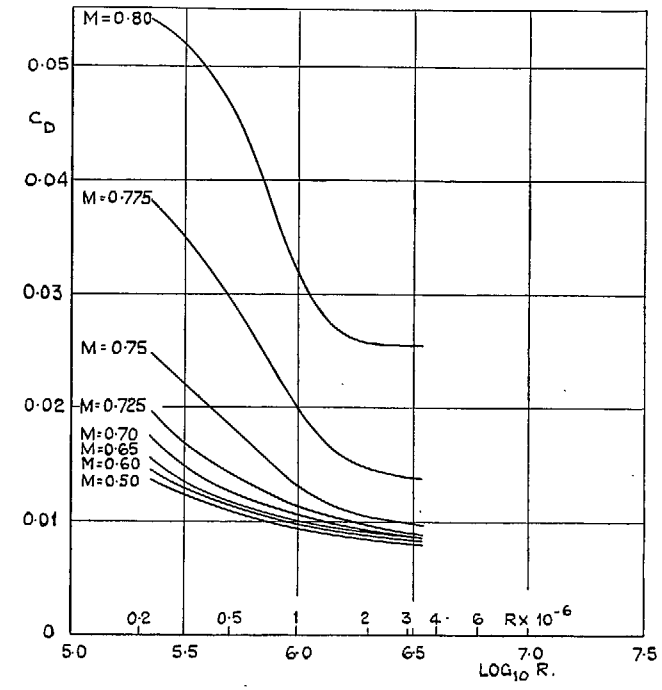

FIG. 21. Scale Effect on Drag Coefficient at High Mach Numbers. (Results fully corrected for wall interference.)

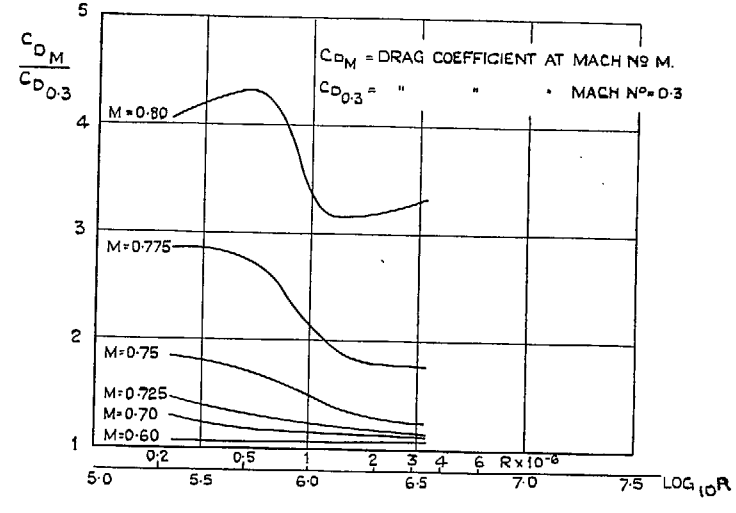

FIG. 22. Scale Effect on Drag Factor. (Results fully corrected for wall interference.)

PRINTED IN GREAT BRITAIN

Publications of the Aeronautical Research Committee

TECHNICAL REPORTS OF THE AERONAUTICAL RESEARCH COMMITTEE—

1934–35 Vol. I. Aerodynamics. 40*s.* (40*s.* 8*d.*)
Vol. II. Seaplanes, Structures, Engines, Materials, etc. 40*s.* (40*s.* 8*d.*)

1935–36 Vol. I. Aerodynamics. 30*s.* (30*s.* 7*d.*)
Vol. II. Structures, Flutter, Engines, Seaplanes, etc. 30*s.* (30*s.* 7*d.*)

1936 Vol. I. Aerodynamics General, Performance, Airscrews, Flutter and Spinning. 40*s.* (40*s.* 9*d.*)
Vol. II. Stability and Control, Structures, Seaplanes, Engines, etc. 50*s.* (50*s.* 10*d.*)

1937 Vol. I. Aerodynamics General, Performance, Airscrews, Flutter and Spinning. 40*s.* (40*s.* 9*d.*)
Vol. II. Stability and Control, Structures, Seaplanes, Engines, etc. 60*s.* (61*s.*)

1938 Vol. I. Aerodynamics General, Performance, Airscrews, 50*s.* (51*s.*)
Vol. II. Stability and Control, Flutter, Structures, Seaplanes, Wind Tunnels, Materials. 30*s.* (30*s.* 9*d.*)

1939 Vol. I. Aerodynamics General, Performance, Airscrews, Engines. 50*s.* (50*s.* 11*d.*)
Vol. II. Stability and Control, Flutter and Vibration, Instruments, Structures, Seaplanes, etc. 63*s.* (64*s.* 2*d.*)

ANNUAL REPORTS OF THE AERONAUTICAL RESEARCH COMMITTEE—

1933–34	1*s.* 6*d.* (1*s.* 8*d.*)
1934–35	1*s.* 6*d.* (1*s.* 8*d.*)
April 1, 1935 to December 31, 1936.	4*s.* (4*s.* 4*d.*)
1937	2*s.* (2*s.* 2*d.*)
1938	1*s.* 6*d.* (1*s.* 8*d.*)
1939-48	*In the press*

INDEXES TO THE TECHNICAL REPORTS OF THE ADVISORY COMMITTEE ON AERONAUTICS—

December 1, 1936 — June 30, 1939.	R. & M. No. 1850.	1*s.* 3*d.* (1*s.* 5*d.*)
July 1, 1939 — June 30, 1945.	R. & M. No. 1950.	1*s.* (1*s.* 2*d.*)
July 1, 1945 — June 30, 1946.	R. & M. No. 2050.	1*s.* (1*s.* 1*d.*)
July 1, 1946 — December 31, 1946.	R. & M. No. 2150.	1*s.* 3*d.* (1*s.* 4*d.*)
January 1, 1947 — June 30, 1947.	R. & M. No. 2250.	1*s.* 3*d.* (1*s.* 4*d.*)

Prices in brackets include postage.

Obtainable from

His Majesty's Stationery Office

York House, Kingsway, LONDON, W.C.2 429 Oxford Street, LONDON, W.1
P.O. Box 569, LONDON, S.E.1
13a Castle Street, EDINBURGH, 2 1 St. Andrew's Crescent, CARDIFF
39 King Street, MANCHESTER, 2 Tower Lane, BRISTOL, 1
2 Edmund Street, BIRMINGHAM, 3 80 Chichester Street, BELFAST

or through any bookseller.